Disorder effects in pnictides : a tunneling spectroscopy study

Y. Noat,* T. Cren, V. Dubost, S. Lange, F. Debontridder, and D. Roditchev

Institut des Nanosciences de Paris, CNRS UMR 7588, Université Pierre et Marie Curie Paris 6,
Campus Boucicaut, 140 rue de Lourmel, F-75015 Paris, France

J. Marcus and P. Toulemonde

Institut Néel, CNRS et Université Joseph Fourier,
25 rue des Martyrs, BP 166, F-38042 Grenoble, France

W. Sacks

Institut de Minéralogie et de Physique des Milieux Condensés, CNRS UMR 7590,
Campus Boucicaut, 140 rue de Lourmel, F-75015 Paris, France
(Dated: July 22, 2010)

We present the synthesis and the tunneling spectroscopy study of superconducting $FeSe_{0.5}Te_{0.5}$ ($T_c = 14$ K), $SmFeAsO_{0.85}$ ($T_c = 45$ K) and $SmFeAsO_{0.9}F_{0.1}$ ($T_c = 52$ K). The samples were characterized by Rietveld refinement of X-ray diffraction patterns and transport measurements. Tunneling experiments on $FeSe_{0.5}Te_{0.5}$ revealed a single superconducting gap ~ 1 meV in BCS-like tunneling conductance spectra. In $SmFeAsO_{0.85}$ and $SmFeAsO_{0.9}F_{0.1}$ however, more complex spectra were observed characterized by two gap-like structures at ~ 4 meV and ~ 10 meV. These spectra are qualitatively understood assuming a two-band superconductor with a 's±' order parameter. We show that depending on the sign relation between the pairing amplitudes in the two bands, the interband quasiparticle scattering has a crucial effect on the shape of the tunneling spectra. Detailed analysis of the tunneling spectroscopy data supports the 's±' model, but single-gap spectra found in $FeSe_{0.5}Te_{0.5}$ are more compatible with a disorder-induced 's'-wave gap, due to the Se-Te substitution.

PACS numbers: 74.25.Gz, 74.72.Jt, 75.30.Fv, 75.40.-s

INTRODUCTION

In 2008, i.e. 22 years after Bednorz and Muller discovery [1] of superconductivity in cuprates, the exciting fining of superconductivity in $LaFeAsO_{1-x}F_x$ ($T_c = 23$ K, reaching $T_c = 43$ K under pressure) [2, 3], gave rise to a completely new family of high-T_c superconductors, with the critical temperature culminating at $T_c = 55$ K in $SmFeAsO_{0.9}F_{0.1}$ [4]. Understanding these materials is of fundamental importance, as one could expect a 'new' and unconventional type of superconductivity to occur there. There exists also a hope in the scientific community that understanding the nature of pairing in iron-based materials could shed light on the complex superconducting (SC) state of the high-T_c cuprates (see the review [5] and refs. therein) where the mechanism is still not fully understood.

As in the cuprates, the iron pnictides have a layered structure and are close to a magnetic transition. The parent compound exhibits magnetism which is destroyed by electron/hole doping, and the SC state ensues. Another analogy with the cuprates is the possible role of strong electronic correlations. However, the parent compound for oxypnictides seems to be a correlated metal rather than an antiferromagnetic Mott insulator. Superconductivity is obtained in this system by charge doping either outside of the FeAs blocks (by O deficiency or F substitution on the O site in the LaFeAsO compound) or directly in the active FeAs planes (by Co substitution for Fe in $BaFe_2As_2$, see for example Sefat et al. [6]). In addition, superconductivity can be induced by mechanical pressure in such systems [7–11], i.e. without introducing chemical disorder.

There is thus a number of questions to be answered. Is the SC state in these compounds unconventional? If yes, what is the SC gap symmetry and the underlying pairing mechanism? Are the iron-pnictides an example of superconductivity mediated by magnetism? What is the nature of the normal state? Does a pseudogap exist in the normal state, i.e. just above T_c, and in the vortex core?

In this paper, we describe the fabrication of $SmFeAsO_{0.85}$ (T_c^{mid}=45 K, [12]), $SmFeAsO_{0.9}F_{0.1}$ (T_c^{mid}=52 K) oxypnictide crystals and FeSe-based SC $FeSe_{0.5}Te_{0.5}$ (T_c^{mid}=12 K) materials. The samples were characterized by temperature-dependent resistivity measurements, Rietveld refinement of X-ray diffraction patterns and finally studied by tunneling spectroscopy (TS) at 4.2 K. While the signature of a single 'BCS-like' gap was observed in tunneling spectra of $FeSe_{0.5}Te_{0.5}$, two 'gap-like' structures, at ~ 3 meV and ~ 10 meV, were revealed in the tunneling conductance spectra of $SmFeAsO_{0.85}$ and $SmFeAsO_{0.9}F_{0.1}$. These structures are interpreted as two SC gaps. Moreover, some local tunneling conductance spectra showed a well-pronounced zero-bias peak - a structure which is absent in the

tunneling DOS of conventional superconductors, but observed in 'd'-wave high-T_c cuprates. In order to give a qualitative understanding of these results, we numerically studied the two-band superconductor in the framework of Schopohl and Scharnberg model [13]. We focused on the influence of interband quasiparticle (QP) scattering on the tunneling DOS in two distinct cases: i - pairing via magnetic coupling ('s$\pm$' model [14]), resulting in a sign reversal between two parts of the SC order parameter (OP) corresponding to two different bands; ii - phonon pairing, with two gaps in the OP having the same phase. Remarkably, we found the interband QP scattering to affect very differently the SC DOS, qualitatively and quantitatively, in these two cases. Within 's$\pm$' model, the QP peaks in the DOS are strongly washed out by the interband QP scattering, while within 's'-wave model, they are much less affected. This difference allowed us to discriminate between two models and to support the 's$\pm$' scenario in the case of SmFeAsO$_{0.85}$ and SmFeAsO$_{0.9}$F$_{0.1}$.

I. PNICTIDES AND IRON CHALCOGENIDES: STRUCTURE, DOPING AND SUPERCONDUCTIVITY

When the SC state is obtained by charge doping of the active FeAs planes, the rare-earth element – oxygen (RE-O) plane acts as a charge reservoir, controlling the carrier concentration in the FeAs planes via the substitution of oxygen by fluorine or via oxygen vacancies. Remarkably, spin fluctuations were observed in SmFeAsO$_{1-x}$F$_x$ (with x=0.18 and 0.3) near the SC transition [15], and magnetic resonance was reported in FeSe$_x$Te$_{1-x}$ [16]. The superconducting OP was shown to be coupled to a magnetic resonance in Ba$_{0.6}$K$_{0.4}$Fe$_2$As$_2$ [17]. These experiments suggest that, in possible analogy to the cuprates, magnetism plays a crucial role in the formation of the SC state. Furthermore, it has been argued that the attractive interaction is mediated by spin fluctuations [14] instead of phonons. As explored in this work, this could lead to a change of sign of the OP between different Fermi sheets [14].

Arsenic high toxicity has motivated the search for other materials with similar structural properties. This led to the discovery of superconductivity in the relatively simple compound FeSe [18] with a critical temperature $T_c = 8$ K, but posing the additional question of chemical disorder. With their similar layered structures, the comparison of the FeAs and FeSe families should be fruitful. As mentioned above, SmFeAsO$_{1-x}$ can be doped either by O deficiency or by F substitution and leaving the FeAs planes pristine. To the contrary, in the FeSe system, where the SC is induced by Se deficiency or by substitution of Se by Te atoms, two different effects are obtained: In the first case, the additional Fe atoms are intercalated between the FeSe planes which thus remain intact upon substitution. The critical temperature reaches 37 K [19–21] or a slightly lower value [22–24] under applied pressure. In the second case, when doping by substitution, the Te atoms are introduced within the FeSe planes and the critical temperature is much lower: ~ 14 K.

To address, at least partially, the question of the SC OP in iron pnictides, we performed tunneling spectroscopy (TS) in the Scanning Tunneling Microscope (STM) geometry. This powerful technique allows local measurements of the QP excitation spectra of superconductors. Indeed, if one of the electrodes is a normal metal (with a constant density of state $N_N(E) \approx const$) and the second one is a superconducting material characterized by an excitation spectrum $N_S(E)$, the derivative of the tunneling current $I(V)$ across such a NIS junction as a function of bias voltage V reads:

$$dI(V)/dV \; \propto \; \int \; N_S\left(E+eV\right)g(E)dE \qquad (1)$$

where $g(E)$ is the derivative of the Fermi-Dirac function $f(E)$: $g(E) = -\partial f(E)/\partial E$; $g(E)$ is a bell-shaped function of width $\sim 3.5 \, kT$. The spectroscopic resolution of the TS is therefore mainly limited by the temperature of the experiment. Since the pioneering experiments by Giaever [25] who measured the SC gap in Pb in planar tunneling junctions, the TS in STM geometry has been successfully used to study conventional (see, for instance, the extensive contributions of Hess et al. [26]) as well as high-Tc superconductors (for a review of STS in cuprates, see [27] and refs. therein).

The above commonly used expression for the tunneling conductance $dI(V)/dV$ neglects the **k**-dependence of the tunneling transparency. Though, the tunneling towards the materials with complex band structure may result in different tunneling probabilities for different parts/sheets of the Fermi surface. The measured tunneling conductance spectra thus probe different portions of the Fermi surface with different spectral weights. This effect, first observed in cuprates [28], was crucial in understanding the two-band superconductivity in MgB$_2$ [29], but also in CaC$_6$ [30] and recently, in Ba$_8$Si$_{46}$ [31]. Thus, the tunneling density of states (DOS) may significantly differ from the QP excitation spectrum of the bulk material.

Despite the large number of experimental studies of FeAs and FeSe-based superconductors, there are relatively few comprehensive TS results. The case of Fe(Se,Te) is maybe the clearer. Indeed, two scanning tunneling spectroscopy studies showed a 's'-wave like single gap superconducting density of states in this material [32, 33]. In their scanning tunneling spectroscopy study of cleaved surfaces of single crystals of the iron chalcogenides Fe$_{1.05}$Se$_{015}$Te$_{0.85}$, Kato et al. [32] found a simple BCS 's'-wave OP, relatively homogeneous, on a spatially inhomogeneous spectral background. Similarly, Hanaguri et al. [33] found a clear s-wave like den-

sity of state in Fe(Se,Te). Nevertheless, basing on quasi-particle scattering interference patterns studies, the authors claim to have evidenced 's±' superconductivity in Fe(Se,Te).

The situation is more complex for FeAs-based materials where more complexe signatures where observed. Millo et al. [34] studied polycrystalline samples of SmFeAsO$_{0.85}$ and, in some regions, observed a gap $\sim$ 8 meV with clear QP peaks; the shape of the tunneling spectra was found compatible with 'd' wave symmetry of the SC OP. In other regions of the sample, a zero bias peak in the conductance spectra was observed. Although the authors suggested a possible 'd'-wave OP, they also remarked that, on a large part of the surface ($\sim 70\%$), TS spectra with a characteristic 'V' shaped background in tunneling conductance were dominant (the conductance increasing almost linearly with the bias voltage, $dI(V)/dV \propto |V|$). Spectra of a very similar shape have already been observed in YBa$_2$Cu$_3$O$_7$ [35] and other cuprates, including the electron-doped case Sm$_{1.85}$Ce$_{0.15}$CuO$_4$ [36].

Pan et al. [37] studied NdFeAs$_{0.86}$F$_{0.14}$ and found two characteristic gaps in spatially separated locations of the sample: a small gap of $\sim$9 meV with a BCS-like shape and temperature dependence, and a larger one $\sim$18 meV having a non-BCS shape. Both gaps were found to close at T_c of the bulk material. In addition, Pan et al. identified a 'pseudogap' opening just above T_c. Yin et al. [38] have observed a gap with well pronounced QP peaks in all locations of studied BaFe$_{1.8}$Co$_{0.2}$As$_2$ sample. The SC nature of the observed gap was proven by vortex imaging under magnetic field; a disordered vortex lattice, attributed to bulk pinning, was reported. Chen et al.[39] found a single BCS-like gap in SmFeAsO$_{0.85}$F$_{0.15}$.

Multigap superconductivity, such as reported by Pan et al. [37], has been suggested for FeAs-based superconductors, as a possible explanation of reported experimental results. Wang et al. [40] explained in this way the point contact spectroscopy data obtained in SmFeAsO$_{1-x}$F$_x$ for $x = 0.1$ and by Daghero et al. [41] for $x = 0.2$ and $x = 0.09$. Indeed, Wang et al. [40] found two gaps, a small one $\Delta_1 = 3.7$ meV and a large gap $\Delta_2 = 10.5$ meV while Daghero et al. [41] found $\Delta_1 = 6.15$ meV and $\Delta_2 = 18$ meV for $x = 0.2$, and $\Delta_1 = 4.9$ meV and $\Delta_2 = 15$ meV for $x = 0.09$ (the typical gap uncertainties being $\sim 10\%$).

Most of these experiments on SmFeAsO compounds suggest a two bands superconductivity scenario with an important QP interband coupling [13], such as observed in MgB$_2$ [42, 43]. Nevertheless, taking into account the presence of magnetic fluctuations in SC iron pnictides, one has to consider a more complex situation, where the SC pairing originates from a magnetic coupling and gives rise to a change of sign between the two 's'-wave parts of the SC OP, as considered in [14].

II. COMPARATIVE CRYSTAL STRUCTURE

As previously mentioned, the pnictide SC state is associated with the FeAs plane, structurally encountered in the natural mineral mackinawite [44] (Fig.1(a)). A vast series of compounds can be designed by different stacking of this plane with other structural units [45] (Fig. 1(b)). In the case of oxypnictides, such as SmFeAsO$_{0.85}$ and SmFeAs(O$_{0.9}$F$_{0.1}$), the carrier doping in the FeAs plane comes from the off-stoichiometry or fluorine substitution in the RE-O plane. In the first case, RE-FeAsO$_{1-\delta}$, the effective doping is 2δ electrons per Fe atom, whereas in the last case RE-FeAs(O$_{1-\delta}$F$_\delta$), it corresponds to δ electrons. In the latter case, one should note that the defect is located *outside* the SC plane and intuitively acts as an additional electrostatic potential. Defects *within* the SC plane can be induced in this family by the substitution of iron atoms by cobalt atoms [46–48].

Concerning the Fe$_{1+y}$Se$_{1-x}$Te$_x$ family (Fig.1(c)), despite a simpler chemical composition, the crystal chemistry of these materials is rather complex, and one should carefully consider the off-stoichiometry when discussing the SC properties [49]. In a perfect stoichiometric compound all Fe atoms, designated Fe(1), are in the tetrahedral sites of the planes. When Fe is present in excess (y>0), it occupies the sites between the Fe(Se, Te) planes, designated as Fe(2). Superconductivity was first discovered in the nominal FeSe$_{0.88}$ Se-deficient compound [18]. It was then demonstrated to correspond to a nearly stoichiometric compound [50], with a T$_c$ of 8 K, and then raised to 34-37 K by applying hydrostatic pressure [19–22]. The substitution of selenium by tellurium was then examined, allowing enhancing T$_c$ to 14 K at ambient pressure [51]. The general tendency throughout the isovalent substitution of selenium by tellurium is the further occupation of the Fe(2) sites between the planes [52]. In this system, the T$_c$ first increases with tellurium substitution with a maximum onset value corresponding to 14 K for the composition FeSe$_{0.5}$Te$_{0.5}$ [53]. The tellurium compound Fe$_{1.07}$Te is non-superconducting [54].

At this stage, one should note important differences between the oxypnictides and iron chalcogenides. First, due to the absence of charge reservoir planes in the latter case, the inter-plane distance is smaller (the inter-plane distance, measured with respect to iron atoms is around 8 Å in the case of oxypnictides, versus 5 Å in the case of iron chalcogenides) and the three-dimensional character is more pronounced. Then, the Se/Te substitution occurs *within* the SC plane, and one could expect strong consequences on the SC properties. The Se/Te disorder may cause an important QP scattering that, in the case of a magnetic fluctuation mediated superconductivity, induces a disorder in the exchange integrals between the iron atoms and, consequently, the scattering by spin density waves. Moreover, the additional inter-plane atom
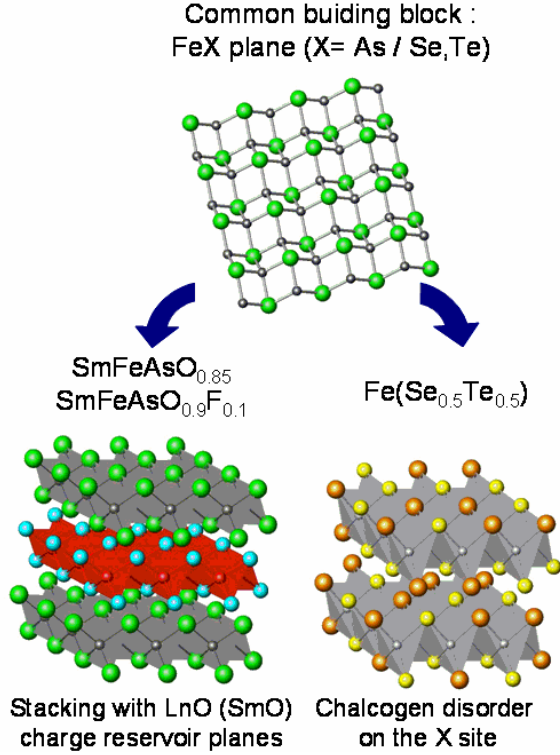
FIG. 1: (Color online) Building-block approach to the crystal chemistry of iron-based superconductors. (a) Superconducting FeX $(X = As, Se)$ plane : Iron(II) is in flattened tetrahedral coordination. (b) Crystal structure of $SmFeAs0_{0.85}$ and $SmFeAs0_{0.90}F_{0.1}$. FeAs planes are alternatively stacked with LnO charge reservoir planes. (c) Crystal structure of $Fe(Se_{0.5}Te_{0.5})$, showing the chemical disorder on the X site $(X = As / Se, Te)$. For this composition, the inter-plane excess iron concentration is almost zero. Color code for (b) and (c). Grey : Fe atoms and Fe-centered polyedra, Green : As atoms, Blue : Sm atoms, Red : oxygen and oxygen-centered polyedra, Se atoms (yellow) are randomly substituted by Te atoms (orange).

Fe(2) is believed to have a magnetic moment, and its influence to the SC state could be more complex than a simple electrostatic potential [55]. Finally, we have chosen for this study single crystals of the composition $FeSe_{0.5}Te_{0.5}$, which correspond to both the highest T_c at ambient pressure $(T_c^{mid} = 12\,K)$, a nearly zero occupation of Fe(2) sites and a maximum Se/Te mixing.

III. FABRICATION AND CHARACTERIZATION OF THE SAMPLES

$SmFeAsO_{0.85}$ and $SmFeAs(O_{0.9}F_{0.1})$ samples (Sm-1111) were prepared under high pressure - high temperature using a "belt" type high pressure cell. Sm, Fe, Fe_2O_3, As and SmF_3 (in the case of the fluorine doped sample) powders were mixed together and pressed in the

FIG. 2: (Color online) Rietveld refinement of $SmFeAsO_{0.9}F_{0.1}$ sample.

form of cylindrical pellets. They were introduced in a home-made boron nitride crucible which was surrounded by a cylindrical graphite resistive heater and the whole assembly was placed in a pyrophyllite gasket. The samples were treated at 6GPa, 1000-1100 °C during 4 hours and then quenched to room temperature. The XRD patterns show that the major phase is the one expected, Sm-1111 with small impurities: FeAs, SmAs and Sm_2O_3, as illustrated in Fig.2. It shows the result of the Rietveld refinement for which the structural parameters of the Sm-1111 phase were refined while only the scaling factor, lattice parameters and profile shape parameters of the secondary phases were refined with atomic positions fixed.

Superconductivity was checked by resistance and a.c. susceptibility measurements. Both show an onset of superconductivity above 50 K (Fig.3) but with a larger transition for the fluorine doped sample (T_c^{mid}=45K for $SmFeAsO_{0.9}F_{0.1}$) compared to the compound with oxygen vacancies (T_c^{mid}=52K for $SmFeAsO_{0.85}$).

Single crystals of $Fe(Se_{0.5}Te_{0.5})$ were fabricated using the sealed quartz tube method. The samples were prepared starting from iron pieces and Se/Te powders mixed together and introduced in a quartz tube which was then sealed under vacuum. The reactants were heated slowly at 500 °C for 10 h, at 950 °C for 5h, slowly cooled down to 350 °C at 5 °C/h and finally quenched in water. Single crystals were extracted mechanically; their resistance (Fig.3b) and magnetization versus temperature were measured. The onset of the SC transition was found at 14 K ($T_c^{mid} = 12$ K) with relatively good transition, i.e. a zero resistance at 10K.

IV. TUNNELING SPECTROSCOPY

We now focus on the TS experiments which were performed in the inverted junction geometry [29, 37]. It is well known that the surface of iron-based pnictides is very

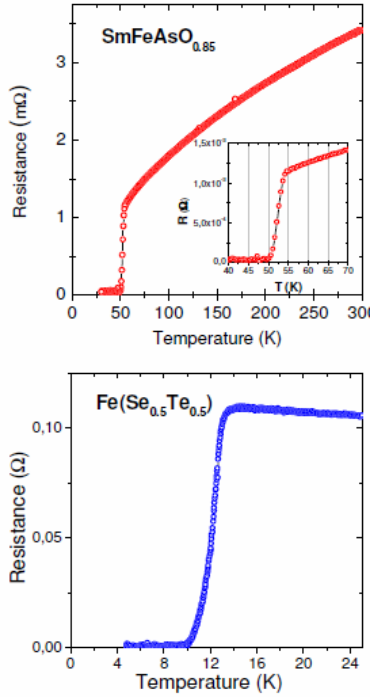FIG. 4: (Color online) Circles: Background corrected tunneling conductance spectrum observed in FeSe$_{0.5}$Te$_{0.5}$ at $T = 4.2$ K, tunneling resistance $R_T = 12.5$ MΩ. Solid line: BCS fit using Dynes formula [56] gives $\Delta = 0.95$ meV; $\gamma = 0.22$ meV. Inset (left): Geometry of the tunneling experiment: small SC crystals were glued on a PtIr tip (and broken in ultra high vacuum before the experiment in order to get a clean surface). A gold crystal was used as the counter electrode. Inset (right): tunneling spectra observed in other studied samples.

FIG. 3: (Color online) a) Resistance versus temperature dependence of polycrystalline SmFeAsO$_{0.85}$ sample (measured by the four terminals method). b) Resistance versus temperature dependence of a FeSe$_{0.5}$Te$_{0.5}$ single crystal (measured by the four terminals method).

reactive and contaminates immediately in air. Hence, in order to limit the contamination the crystals effects in TS experiments, the samples were broken in UHV. In practice, small pnictide crystals were glued to the apex of Pt-Ir STM tips (as illustrated in inset of Fig.4) with conducting silver glue and introduced in UHV chamber containing the STM unit. The crystals were then broken under ultra-high vacuum conditions. A pure gold surface was used as the counter-electrode. For each composition a large number of samples have been studied.

Typical tunneling conductance spectra of FeSe$_{0.5}$Te$_{0.5}$ are presented in inset of Fig.4. The spectra clearly show a single gap at zero bias followed by broad peaks on each side. A weak spectral background is observed; it varies from one sample to another. Once this background substracted, the spectra may be well fitted considering 's'-wave BCS excitation spectrum with finite QP lifetime (Dynes formula, ref. [56]) as shown on Fig.4. The fits of different spectra give a gap value of $\sim 1.0 \pm 0.1$ meV. Note that it is smaller than the expected value (1.9 meV) expected for a conventional BCS superconductor for which $2\Delta/kT_c \approx 3,52$. It is important to note the large value of the broadening parameter $\gamma \sim 0.2$ meV, varying from one sample to another. These observations of a single-gap shape of the spectra are in good agrement with previous

tunneling experiments [32, 33]. Nevertheless, the gap value we found is clearly smaller than the 2 mev found by Kato et al. [32] and the 1,7 meV found by Hanaguri et al. [33]. At this moment, we have no clear explanation for this discrepancy. Thus, while the existence of a single gap in FeSe$_{0.5}$Te$_{0.5}$ was clearly established, the spectral broadening did not allow us to distinguish definitively between a simple 's'-wave or a more complex OP in this materials. Indeed, basing on quasiparticle interference patterns observed by scanning tunneling spectroscopy Hanaguri et al. [33] suggested an unconventional 's±' order parameter for this material.

The tunneling conductance data observed in SmFeAsO$_{0.85}$ (Fig.5(left panel)) and SmFeAsO$_{0.9}$F$_{0.1}$ (Fig.6(left panel)) are very different from the simple BCS-like case of FeSe$_{0.5}$Te$_{0.5}$. A large number of spectra exhibit two 'gap-like' structures at respectively $\sim 3 - 4$ meV and ~ 10 meV. The largest gap is defined by a kink around $\sim 10 \pm 3$ meV (dashed bands in Figs.5,6 (left panel)) while the low energy gap is directly seen in the spectra near zero-bias, surrounded by two peaks at $\sim 4 \pm 1$ meV (dashed line in Figs. 5,6 (left panel)). Both spectroscopic features are observed on a 'V' shaped background varying from one sample to other. Such a background could be related to the electronic surface states resulting from dangling bonds or to the existence of a correlated metal. A few spectra exhibit a zero bias peak (Figs.5,6 (right panel)). All spectroscopic features we observed - two gaps, the 'V' shaped background and the presence of a zero bias peak, are in complete agreement with the findings of Millo et al. [34].

FIG. 5: (Color online) Tunneling spectra of $SmFeAsO_{0.85}$ acquired at T =4.2 and at tunneling resistance R_T=12.5MΩ . Left panel: two gap-like structures at respectively at ~10mV and ~3mV a) superimposed on a 'V' shaped background are clearly visible. Dashed lines and bands are put at characteristic bias values. Right panel: selected spectra exhibiting a zero bias peak.
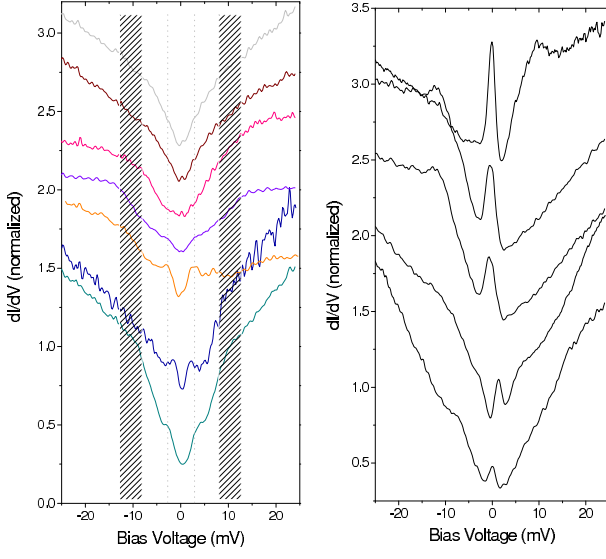

FIG. 6: (Color online) Tunneling spectra of $SmFeAsO_{0.9}F_{0.1}$ acquired at T =4.2 and at tunneling resistance R_T=12.5MΩ . Left panel: two gap-like structures at respectively at ~11mV and ~4mV a) superimposed on a 'V' shaped background are clearly visible. Dashed lines and bands are put at characteristic bias values. Right panel: selected spectra exhibiting a zero bias peak.

V. INTERPRETATION OF THE RESULTS

The two gap-like structures in the spectra of $SmFeAsO_{0.85}$ and $SmFeAsO_{0.9}F_{0.1}$ strongly suggest the existence of two SC gaps in these materials. Mazin et al. [14] have proposed that a magnetic coupling could be the 'glue' for superconductivity, which would make the pnictides very different from other multi-gap superconductors as, for instance, the double-gap SC state in MgB_2. In order to distinguish between the two situations, it is helpful to reconsider the problem of two-gap superconductivity and, specifically, the QP interband scattering effects.

Two-gap model of Suhl

As shown by Suhl, Matthias, and Walker (SMW) [57], the one-band isotropic BCS model can be extended to the case of two energy bands. In their description, a Cooper pair can absorb a phonon and be scattered either in the same band or in the other band. The hamiltonian is the sum of the kinetic energy $H_K = \sum_{k\sigma} \epsilon_k c_{k\sigma}^+ c_{k\sigma} + \epsilon_k d_{k\sigma}^+ d_{k\sigma}$ and of the partial hamiltonians describing the intraband pair scattering in each band, H_{11} and H_{22} and the interband pair scattering H_{12}:

$$H_{11} = V_{11} \sum_{kk'} c_{k\uparrow}^+ c_{-k\downarrow}^+ c_{-k'\downarrow} c_{k'\uparrow}$$

$$H_{22} = V_{22} \sum_{kk'} d_{k\uparrow}^+ d_{-k\downarrow}^+ d_{-k'\downarrow} d_{k'\uparrow}$$

$$H_{12} = V_{12} \sum_{kk'} c_{k\uparrow}^+ c_{-k\downarrow}^+ d_{-k'\downarrow} d_{k'\uparrow} + d_{k\uparrow}^+ d_{-k\downarrow}^+ c_{-k'\downarrow} c_{k'\uparrow}$$

where c^+, c, d^+, d are the corresponding creation and annihilation operators in each band, V_{11} and V_{22} are the intraband coupling potential corresponding to absorption or emission of a phonon with a pair scattering in the same band, V_{12} is the interband pair coupling corresponding to the scattering of a Cooper pair from one band to the other.

This model gives rise to two gaps in the excitation spectrum, Δ_1 and Δ_2, which are defined by two coupled equations:

$$\begin{cases} \Delta_1[1 - V_{11}N_1 F(\Delta_1)] = \Delta_2 V_{12} N_2 F(\Delta_2) \\ \Delta_2[1 - V_{22}N_2 F(\Delta_2)] = \Delta_1 V_{12} N_1 F(\Delta_1) \end{cases} \quad (2)$$

where $N_i = N_i(E_F)$, $i = 1,2$, is the normal state DOS at the Fermi level in each band. $F(\Delta_i)$ (i =1,2) is a function depending on the temperature T, ω_0 is the cutoff frequency for the mechanism responsible for the coupling (i.e. the Debye frequency in the case of a phonon coupling):

$$F(\Delta) = \int_0^{\hbar\omega_0} Re\left\{ d\epsilon \tanh\left[\frac{\sqrt{\epsilon^2 + \Delta^2}}{2k_B T}\right] / \sqrt{\epsilon^2 + \Delta^2} \right\} \quad (3)$$

If the interband pair coupling parameter term V_{12} is neglected, one obtains a superposition of two SC condensates with two critical temperatures and a DOS which is the sum of two BCS-type DOS. Otherwise ($V_{12} \neq 0$), one gets two gaps which close at the same critical temperature depending on different parameters of the model. This is the situation suggested for MgB$_2$ [42]. However, to account for the observed SC behavior of this material [43], the Cooper pair scattering is not enough, and the QP scattering effects must be additionally considered [13].

Two gap superconductor with sign reversal

Mazin et al. [14] considered a more odd situation where the pairing originates from a magnetic coupling, and the interband pair scattering parameter V_{12} becomes negative. Consequently, the two components of the SC OP, characterized by two gaps in the excitation spectrum, have opposite signs. Mazin et al. proposed that such a situation could exist in the pnictides. When the intraband coupling can be neglected compared to the interband coupling, i.e. when $V_{11}, V_{22} \ll |V_{12}|$, then the SMW Eqs.2 for the two gaps simplify. At zero temperature, and assuming that the cutoff frequency of the coupling mechanism is much larger than the gap amplitude $\omega_0 \gg \Delta_{1,2}$, one obtains:

$$\begin{cases} \Delta_1 = \Delta_2 V_{12} N_2 ln\left(\frac{2\hbar\omega}{\Delta_1}\right) \\ \Delta_2 = \Delta_1 V_{12} N_1 ln\left(\frac{2\hbar\omega}{\Delta_2}\right) \end{cases} \quad (4)$$

Therefore, it appears that in such a situation the gap in the first band is determined mainly by the DOS in the other band. The gap ratio at zero temperature is approximately given by $(\Delta_1/\Delta_2)^2 \sim N_2/N_1$.

Effect of quasiparticle scattering on the DOS

Schopohl and Scharnberg [13] considered, in addition to SMW approximation, a term allowing the QPs to be scattered from one band to the other. This Schopohl-Scharnberg model (SSM) of a two-gap SC is formally equivalent to the Mc Millan model [58] describing the normal metal - superconductor proximity effect in real space. When taking into account the interband QP scattering, not accounted for in SMW model (Eq. 2), the energy gaps $\Delta_i(E)$ (where $i =$ 1, 2) become energy dependent and are given by two coupled equations:

$$\Delta_1(E) = \frac{\Delta_1^0 + \Gamma_{12}\Delta_2(E)/\sqrt{\Delta_2^2(E) - (E - i\Gamma_{21})^2}}{1 + \Gamma_{12}/\sqrt{(\Delta_2^2(E) - (E - i\Gamma_{21})^2)}} (5)$$

$$\Delta_2(E) = \frac{\Delta_2^0 + \Gamma_{21}\Delta_1(E)/\sqrt{\Delta_1^2(E) - (E - i\Gamma_{12})^2}}{1 + \Gamma_{21}/\sqrt{(\Delta_1^2(E) - (E - i\Gamma_{12})^2)}}$$

where $\Gamma_{12} = \hbar/\tau_{12}$ and $\Gamma_{21} = \hbar/\tau_{21}$ are the scattering coefficients and τ_{ij} represent the QP lifetimes in each band. Δ_1^0 and Δ_2^0 are the gaps obtained from the self-consistency equations:

$$\Delta_i^0 = \lambda_{ii} \int_0^{\hbar\omega_i} \mathrm{d}E \tanh\left[\frac{E}{2k_BT}\right] \mathrm{Re}\left[\frac{\Delta_i(E)}{\sqrt{E^2 - \Delta_i^2(E)}}\right]$$
$$+ \lambda_{ij}\sqrt{\frac{N_j}{N_i}} \int_0^{\hbar\omega_{ij}} \mathrm{d}E \tanh\left[\frac{E}{2k_BT}\right] \mathrm{Re}\left[\frac{\Delta_i(E)}{\sqrt{E^2 - \Delta_i^2(E)}}\right] \quad (6)$$

where i=(1,2) and $\lambda_{ii} = V_{ii}N_i$ are the intraband electron-phonon coupling constants, while $\lambda_{ij} = V_{ij}\sqrt{N_iN_j}$ is the interband electron-phonon coupling constant of the SMW model. The partial DOSs $N_S^i(E)$ corresponding to the two different bands $i = 1, 2$ are obtained by inserting the energy dependent gaps $\Delta_1(E)$ or $\Delta_2(E)$ in the standard BCS expression for the DOS [59]:

$$N_S^i(E) = \mathrm{Re}\left[\frac{|E|}{\sqrt{E^2 - \Delta_i(E)^2}}\right] \quad (7)$$

Following Mazin et al. [14], we considered that the energy gaps in each band have opposite signs ('s±' model). We further developed SSM approach to this 's±' approximation. We have then calculated the partial DOS in each band in 's±' case, for different values of the interband QP scattering parameters Γ_{ij}. We finally compared the effects of QP scattering on SC DOS within 's'-wave two-band SSM [60] and 's±' SSM model. The results of our calculations, done for $\Delta_1^0 = \pm3$meV (small initial gap) and $\Delta_2^0 = 8$meV (large initial gap), are presented in Fig.7, for different amplitudes of the QP interband scattering Γ_{ij}. In the 's'-wave two-gap SSM case (Fig.7(left panel)), the partial DOS $N_S^{1,2}(E)$ (corresponding, respectively, to small and large gap bands 1 and 2) are relatively weakly affected by increasing QP interband scattering. However, in the 's±' SSM case (Fig.7(right panel)) the interband QP scattering has a dramatic effect on the partial DOS. Both the small gap and the large gap partial DOS ((Figs.7(c) and (d), respectively) show rapid filling with the states inside initial gaps. The effect is particularly strong for the large gap DOS, since for a high enough value of the interband QP scattering parameter Γ_{21}, the QP peaks at the large gap energy almost disappear in the DOS (Fig.7(d)). In such a case, the large gap can be hardly distinguished in the tunneling conductance spectra (Fig.7(f)).

In order to compare the calculated DOS to the TS data, one has to take into account the **k**-selectivity in the tunneling process [28, 29]. The simplest way is to consider that some part T_1 of tunneling electrons go to the band $i = 1$ where the gap $\Delta_1(E)$ (small gap) exists whereas the rest of electrons $T_2 = 1 - T_1$ tunnel to the band $i = 2$ characterized by the gap $\Delta_2(E)$ (large gap). Such an approximation gives the tunneling DOS
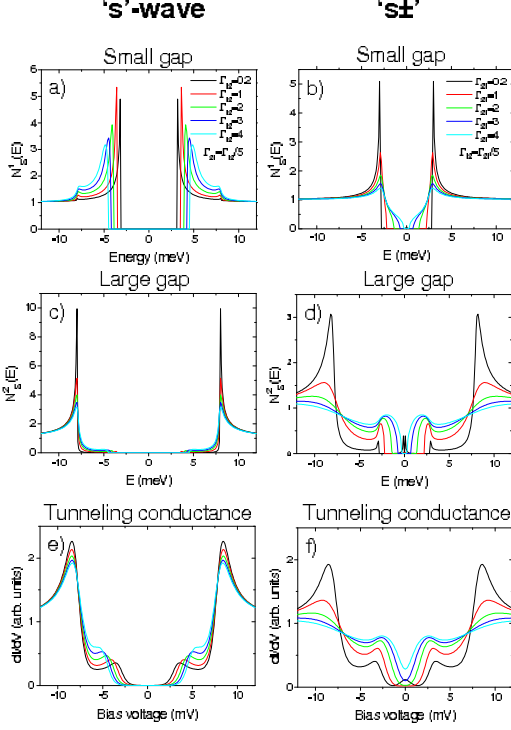
FIG. 7: (Color online) Left panel: Partial DOS, $N_S^1(E)$ (a) and $N_S^2(E)$ (c) calculated within 's'-wave SSM model for various QP interband scattering rates Γ_{12} =0.2, 1, 2, 3, 4meV; Γ_{21}/Γ_{12} =5. The starting gap parameters are Δ_1^0 =3meV, Δ_2^0 =8meV. (e) - corresponding tunneling conductance calculated for T =4.2K using the tunneling weights T_1 =0.8, T_2 =0.2.
Right panel: Partial DOS, $N_S^1(E)$ (b) and $N_S^2(E)$ (d) calculated within 's$\pm$' SSM model for various QP interband scattering rates. All parameters are kept the same as in 's'-wave case (left panel) except Δ_1^0 which is of opposite sign, Δ_1^0 =-3meV. (f) - corresponding tunneling conductance calculated for T =4.2K using the tunneling weights T_1 =0.8, T_2 =0.2.

as a weighted sum of two partial SSM DOS (Eq.7):

$$N_S^{eff}(E) = T_1 N_S^1(E) + T_2 N_S^2(E), \qquad (8)$$

with $T_1 + T_2 = 1$. The tunneling conductance at finite temperature is then obtained by replacing the term $N_S(E + eV)$ by $N_S^{eff}(E + eV)$ in the integral $dI(V)/dV$ (Eq.1). The resulting curves, calculated for $T_1 = 0.8$, $T_2 = 0.2$, are presented in Fig.7(e) and Fig.7(f), respectively for 's'-wave and 's$\pm$' situations. We point out on a striking difference between two results, specifically at high enough QP scattering rates ($\Gamma_{12} \geq 1$), where the large gap peaks (at $\sim \pm 8$ mV) are suppressed and only some kinks remain. Remarkably, the QP peaks due to the small gap are very robust: They remain clearly visible at any studied value of Γ_{ij}.

VI. DISCUSSION AND PERSPECTIVES

It is tempting to compare the effects of disorder in pnictides and chalcogenides to high-T_c cuprates. In cuprates, it has been shown that two main types of disorder can be distinguished, having drastically different effects: in plane disorder in the CuO_2 layer and out of plane disorder (see for instance ref. [61] and ref. therein). Weak disorder consists in substitution of atoms belonging to the charge reservoir planes (*out of plane disorder*), whereas strong disorder corresponds to oxygen vacancies or copper substitution by zinc or nickel (*in plane disorder*). The former is known to induce spatial inhomogeneities in the superconducting state and a pseudogap in the excitation spectrum [62], whereas the latter is far more detrimental to superconductivity. As an example, a few percent of Zn decreases the critical temperature even though it is non magnetic [63] and causes gapless SC [64].

At first glance, the concepts developed for the cuprates can be extented to the case of iron-based superconductors. Indeed, we can define in the same spirit *in plane* and *out of plane* disorder, with respect to the FeAs plane. However, making direct comparison between pnictides (LnFeAsO) and chalcogenide (FeSe) is not straightforward since, contrary to iron pnictides and cuprates, a charge reservoir plane does not exist, strictly speaking, in the iron chalcogenides family.

Based on the fact that the experimental spectra in $SmFeAsO_{0.85}$ and $SmFeAsO_{0.9}F_{0.1}$ are quite similar, we first suggest that the SC properties are relatively insensitive to the nature of out of plane dopants. The situation is drastically different for in plane doping. The effect of in plane disorder is complex since, as shown in the literature, doping by substitution depends on the nature of the substituting atoms, isovalent or non-isovalent: The doping can be induced in the LnFeAsO family by non-isolectronic substitutions of iron by cobalt and nickel in the FeAs plane. In this case, the superconducting region is dome-like with optimal T_c of 13 K for a doping level $x_{Co} = 0.075$ in $LaFe_{1-x}Co_xAsO$ [48][46]. Hence, the superconductivity appears robust with respect to strong *in plane* disorder. However, we point out that the order of magnitude of the T_c remains in the range of what is expected for conventional superconductivity. On the other hand, isovalent doping such as subtitution of As by Phosporous in $LaFeAs_{1-x}P_xO$ leads to superconductivity with a reduced temperature ($T_c^{mid} \sim 10.8$ K for the optimally doped x =0.25–0.3) [65]. Those different results suggest that one has to distinguish between doping effects (for non-isovalent substitution) and disorder effects (for isovalent substitution).

Our simulations show that the effect of QP scattering in 's$\pm$' case (i.e. in the case of a magnetic coupling) is very different from the 's'-wave situation. Accordingly, the disorder in FeAs (FeSe) plane should lead to destruc-

tive interferences in the 's±' case, and only an remaining 's'-wave phononic superconductivity would survives. This point should be further confirmed experimentally, for example, by a decrease of the magnon frequency when the active planes are affected. If observed, this would confirm our guess: Out of plane defects in oxypnictides $SmFeAsO_{0.85}$ and $SmFeAsO_{0.9}F_{0.1}$ do not affect strongly the SC OP and preserve both the magnetic coupling and the two-gap structure.

In the case of Fe(Se,Te), the substitution of Se by Te should give rise to a strong disorder, i.e. more precisely to a strong interband quasiparticle scattering that would destroy the 's±' SC OP, resulting in a single 'BCS-type' SC gap (this occurs if V_{11} and V_{22} are non-zero). From our full self-consistent calculations [66] we infer that even a very small amount of Te would probably be enough to suppress the 's±' SC OP. This scenario is not in agreement with Hanaguri et al. [33] who claim to observe 's±' superconductivity in Fe(Se,Te). The fact that neutron scattering experiments show a resonance at 6∼meV in the magnetic scattering at the antiferromagnetic wave vector Q=(0.5, 0.5), which intensity increases abruptly when the sample is cooled below T_c [16] is also in favor of a 's±' scenario [67]. The only possibility for a sign-reversal 's±' order parameter in $FeSe_{0.5}Te_{0.5}$ would be that Te substitution does not induce strong interband quasiparticle scattering. Nevertheless, we see a neat difference between $SmFeAsO_{0.85}$ and $FeSe_{0.5}Te_{0.5}$. In $SmFeAsO_{0.85}$ we observed a strongly damped double gap together with frequent zero-bias peaks (Figs.5 and 6); both are well explained in a 's±' scenario. On the other hand, in the case of $FeSe_{0.5}Te_{0.5}$, a simple 's'-wave like gap is observed and no zero-bias peaks are present; both facts plead for a simple BCS mechanism.

Apart from substituting Se by Te atoms, doping in FeSe is also possible with interplane Fe atoms, such as in $Fe_{1+\delta}Se$ (which is also sometimes written as Fe_xFeSe). Such a doping might have a different effect. In this case, FeSe planes are preserved, the doping being provided by the excess of Fe localized in between them. This hypothesis seems to be confirmed by thermal conductivity measurements by Dong et al. [68] which are favorable to a nodeless multigap SC OP in $Fe_{1+\delta}Se$. Moreover, the search for a double gap structure in $Fe_{1+\delta}Se$ by TS is of immediate interest in order to understand the nature of the superconducting coupling in this material. The impressive increase of T_c with pressure observed in $Fe_{1+\delta}Se$ which can reach 37K [19–24, 69], is most probably related to the evolution of the strength of the SC pairing mechanism (presumably of magnetic origin) with pressure. On the other hand, the $FeSe_{1-x}Te_x$ saturates to ∼ 20K in thin films with epitaxial pressure [70] and in the bulk [71], a value compatible with a conventional phononic superconductivity. The *isolectronic* substitution of iron by ruthenium and non isoelectronic substitution of iron by cobalt atoms, which both induces a

strong *in plane* disorder, lead to a dramatic decrease of T_c in $NdFe_{1-y}M_yAsO_{0.89}F_{0.11}$ (M=Co, Ru) which drops from ∼48 K for x=0 to 0 K (non-superconducting phase) above x=0.13 [72]. Such results strongly support our idea about the fragility of the 's±' SC OP with respect to the disorder strength.

In view of our findings, one can also expect that substitution of iron by nickel or cobalt in $LnFe_2As_2$ family will lead to a single gap structure.

VII. CONCLUSION

In conclusion, we have synthesized iron-based superconductors $FeSe_{0.5}Te_{0.5}$ ($T_c = 14$ K), $SmFeAsO_{0.85}$ ($T_c = 45$ K) and $SmFeAsO_{0.9}F_{0.1}$ ($T_c = 52$ K) and performed tunneling spectroscopy of them at 4.2 K and in ultra-high vacuum. In $FeSe_{0.5}Te_{0.5}$ crystals we observed a single 'BCS-like' gap while in $SmFeAsO_{0.85}$, $SmFeAsO_{0.9}F_{0.1}$ the tunneling spectra revealed two energy scales which we associate with a multigap superconductivity in these materials. The tunneling conductance spectra can be qualitatively understood within a 's±' two-gap model considering the sign reversal in the OP, due to a magnetic pairing. We showed that the 's±' SC DOS is dramatically affected by QP interband scattering, in contrast to the case of a 's'-wave two-gap superconductivity, which was found much more robust. One of the possible explanations of the observed single gap DOS in $FeSe_{0.5}Te_{0.5}$ could be in the suppression of the 's±' superconductivity there by strong disorder resulting from the Se-Te substitution.

---

* Electronic address: yves.noat@insp.jussieu.fr

[1] Bednorz J. G. and Muller K. A., Z. Phys. B. **64**, 189 (1986).

[2] Y. Kamihara, T. Watanabe, M. Hirano, H. Hosono, J. Am. Chem. Soc. **130**, 3296 (2008).

[3] H. Takahashi, K. Igawa, K. Arii, Y. Kamihara, M. Hirano and H. Hosono, Nature **453** 376 (2008).

[4] Z.-A. Ren, W. Lu, J. Yang, W. Yi, X.-L. Shen, Z.-C. Li, G.-C. Che, X.-L. Dong, L.-L. Sun, F. Zhou, Z.-X. Zhao, Chin. Phys. Lett. **25**, 6 2215 (2008).

[5] Patrick A. Lee, Naoto Nagaosa and Xiao-Gang Wen, Review of Modern Physics, **78**, 17 (2006).

[6] Athena S. Sefat, Rongying Jin, Michael A. McGuire, Brian C. Sales, David J. Singh, and David Mandrus, Phys. Rev. Lett. **101**, 117004 (2008).

[7] Milton S. Torikachvili, Sergey L. Bud'ko, Ni Ni, and Paul C. Canfield, Phys. Rev. Lett. **101**, 057006 (2008)

[8] H.Okada, K. Igawa, H.Takahashi, Y. Kamihara, M. Hirano, H. Hosono, K. Matsubayashi, and Y. Uwatoko, Journal of the Physical Society of Japan **77**, 113712 (2008).

[9] Patricia L. Alireza , Y. T. Chris Ko , Jack Gillett , Chiara M. Petrone , Jacqueline M. Cole , Gilbert G. Lonzarich and Suchitra E. Sebastian, J. Phys.: Condens. Matter **21** 012208 (2009).

[10] K. Matsubayashi et al., N. Katayama, K. Ohgushi, A. Yamada, K. Munakata, T. Matsumoto, Y. Uwatoko, J. Phys. Soc. Jpn. **78**, 073706 (2009).

[11] K. Igawa, H. Okada, H. Takahashi, S. Matsuishi, Y. Kamihara, M. Hirano, H. Hosono, K. Matsubayashi, and Y. Uwatoko, J. Phys. Soc. Jpn. **78** 025001 (2009).

[12] T_c^{mid} is defined at the half of the resistive superconducting transition.

[13] N. Schopohl and K. Scharnberg, Solid State Commun. **22** 371 (1977).

[14] I. I. Mazin, D. J. Singh, M. D. Johannes, and M. H. Du, Phys. Rev. Lett. **101**, 057003 (2008).

[15] A. J. Drew, F. L. Pratt, T. Lancaster, S. J. Blundell, P. J. Baker, R. H. Liu, G. Wu, X. H. Chen, I. Watanabe, V. K. Malik, A. Dubroka, K. W. Kim, M. Rössle, and C. Bernhard, Phys. Rev. Lett. **101**, 097010 (2008); A. J. Drew, Nature Mater. **8**, 310 (2009).

[16] Yiming Qiu, Wei Bao, Y. Zhao, Collin Broholm, V. Stanev, Z. Tesanovic, Y. C. Gasparovic, S. Chang, Jin Hu, Bin Qian, Minghu Fang, and Zhiqiang Mao, Phys. Rev. Lett. **103**, 067008 (2009); J. Wen et al., Phys. Rev. B 81, 100513(R) (2010).

[17] A. D. Christianson et al., Nature **456**, 930 (2008).

[18] F.C. Hsu, J.Y. Luo, K.W. Yeh, T.K. Chen, T.W. Huang, P.M. Wu, Y.C. Lee, Y.L. Huang, Y.Y. Chu, D.C. Yan, M.K. Wu, Proc. Natl. Acad. Sci. USA **105**, 14262, (2008).

[19] S. Medvedev, T. M. McQueen, I. A. Troyan, T. Palasyuk, M. I. Eremets, R. J. Cava, S. Naghavi, F. Casper, V. Ksenofontov, G. Wortmann, C. Felser, Nature mat. **8**, 630 (2009).

[20] S. Margadonna, Y. Takabayashi, Y. Ohishi, Y. Mizuguchi, Y. Takano, T. Kagayama, T. Nakagawa, M. Takata, and K. Prassides, Phys. Rev. B **80**, 064506 (2009).

[21] V. A. Sidorov, A. V. Tsvyashchenko and R. A. Sadykov, J. Phys.: Condens. Matter **21**, 415701 (2009).

[22] G. Garbarino, A. Sow, P. Lejay, A. Sulpice, P. Toulemonde, M. Mezouar and M. Nùñez-Regueiro, Europhys. Lett. **86** 27001 (2009).

[23] Yoshikazu Mizuguchi, Fumiaki Tomioka, Shunsuke Tsuda, Takahide Yamaguchi, and Yoshihiko Takano, Appl. Phys. Lett. **93**, 152505 (2008).

[24] Kiyotaka Miyoshi, Yuta Takaichi, Eriko Mutou, Kenji Fujiwara, and Jun Takeuchi, J. Phys. Soc. Jpn. **78**, 093703 (2009).

[25] I. Giaever, Phys. Rev. Lett. **5**,147 (1960).

[26] H. F. Hess, R. B. Robinson, and J. V. Waszczak, Phys. Rev. Lett. **64**, 2711 (1990).

[27] Øystein Fischer, M. Kugler, I. Maggio-Aprile, C. Berthod and C. Renner, Review of Modern Physics, **79**, 353 (2007).

[28] P. Mallet, D. Roditchev, W. Sacks, D. Défourneau, and J. Klein, Phys. Rev. B, **54**, 13324 (1996).

[29] F. Giubileo, D. Roditchev, W. Sacks, R. Lamy, D. X. Thanh, J. Klein, S. Miraglia, D. Fruchart and J. Marcus and Ph. Monod, Phys. Rev. Lett. **87**, 177008 (2001).

[30] N. Bergeal, V. Dubost, Y. Noat, W. Sacks, D. Roditchev, N. Emery, C. Hérold, J-F. Marêché, P. Lagrange and G. Loupias, Phys. Rev. Lett. **97**, 077003 (2006).

[31] Y. Noat, T. Cren, P. Toulemonde, A. San Miguel, F. Debontridder, V. Dubost and D. Roditchev. Phys. Rev. B, **81**, 104522 (2010).

[32] Takuya Kato, Yoshikazu Mizuguchi, Hiroshi Nakamura, Tadashi Machida, Hideaki Sakata and Yoshihiko Takano, Phys. Rev. B **80**, 180507(R) (2009)

[33] N T. Hanaguri, S. Niitaka, K. Kuroki, H. Takagi, Science **328**, 474 (2010).

[34] Oded Millo, Itay Asulin, Ofer Yuli, Israel Felner, Zhi-An Ren, Xiao-Li Shen, Guang-Can Che, and Zhong-Xian Zhao , Phys. Rev. B **78**, 092505 (2008).

[35] T. Cren, D. Roditchev, W. Sacks and J. Klein, Europhys. Lett. **52**, 203 (2000).

[36] A. Zimmers, Y. Noat, T. Cren, W. Sacks, D. Roditchev, B. Liang, and R. L. Greene, Phys. Rev. B **76**, 132505 (2007).

[37] M.H. Pan, X.B. He, G. Li, J.F. Wendelken, R. Jin, A.S. Sefat, M.A. McGuire, B.C. Sales, D. Mandrus, E.W. Plummer, arXiv:0808.0895 (2008).

[38] Yi Yin, M. Zech, T. L. Williams, X. F. Wang, G. Wu, X. H. Chen and J. E. Hoffman, Phys. Rev. Lett. **102**, 097002 (2009).

[39] T. Y. Chen, Z. Tesanovic, R. H. Liu, X. H. Chen and C. L. Chien, Nature **453** 1224 (2008).

[40] Yong-Lei Wang, Lei Shan, Lei Fang, Peng Cheng, Cong Ren and Hai-Hu Wen, Supercond. Sci. Technol. **22**, 015018 (2009).

[41] D. Daghero, M. Tortello, R. S. Gonnelli, V. A. Stepanov, N. D. Zhigadlo and J. Karpinski, Phys. Rev B **80**, 060502(R) (2009).

[42] Amy Y. Liu, I. I. Mazin, and Jens Kortus, Phys. Rev. Lett. **87**, 087005 (2001).

[43] H. Schmidt, J.F. Zasadzinski, K.E. Gray and D.G. Hinks, Physica C **385**, 221 (2003).

[44] H. Strunz, E. N. Nickel, Strunz mineralogical tables, 9 th edition, E. Schweizenbart (2001).

[45] Z.-A. Ren, Z.-X. Zhao, Adv. Mater. **21**, 4584 (2009).

[46] A. S. Sefat, A. Huq, M. A. McGuire, R. Jin, B. C. Sales,D. Mandrus, L. M. D. Cranswick, P. W. Stephens, K H. Stone, Phys. Rev. B **78**, 104505, (2008).

[47] Yanpeng Qi, Zhaoshun Gao, Lei Wang, Dongliang Wang, Xianping Zhang and Yanwei Ma, Supercond. Sci. Technol. **21**, 115016 (2008).

[48] C. Wang, Y. K. Li, Z. W. Zhu, S. Jiang, X. Lin, Y. K. Luo, S. Chi, L. J. Li, Z. Ren, M. He, H. Chen, Y. T. Wang, Q. Tao, G. H. Cao, Z. A. Xu, Phys. Rev. B **79**, 054521, (2009).

[49] T. M. McQueen, Q. Huang, V. Ksenofontov, C. Felser, Q. Xu, H. Zandbergen, Y. S. Hor, J. Allred, A. J. Williams, D. Qu, J. Checkelsky, N. P. Ong, R. J. Cava, Phys. Rev. B **79**, 014522 (2009)

[50] A. J. Williams, T. M. McQueen, R. J. Cava, Solid State Com. **149**, 1507 (2009).

[51] M. H. Fang, H. M. Pham, B. Qian, T. J. Liu, E. K. Vehstedt, Y. Liu, L. Spinu, and Z. Q. Mao, Phys. Rev. B **78**, 224503 (2008), K. W. Yeh, T. W. Huang, Y. L. Huang, T. K. Chen, F. C. Hsu,,Phillip M. Wu, Y. C. Lee, Y. Y. Chu, C. L. Chen, J. Y. Luo, D. C.Yan, and M. K. Wu, Europhys. Lett. **84**, 37002 (2008).

[52] B. C. Sales, A. S. Sefat, M. A. McGuire, R. Y. Jin, D. Mandrus, Y. Mozharivskyj, Phys. Rev. B **79**, 094521 (2009)

[53] M.K. Wu, F.C. Hsu, K.W. Yeh, T.W. Huang, J.Y. Luo, M.J. Wang, H.H. Chang, T.K. Chen, S.M. Rao, B.H. Mok, C.L. Chen, Y.L. Huang, C.T. Ke, P.M. Wu, A.M. Chang, C.T. Wu, T.P. Perng, Physica C **469**, 340 (2009)

[54] D. Fruchart, P. Convert, P. Wolfers, R. Madar, J. P. Senateur, and R. Fruchart, Mater. Res. Bull. **10**, 169 (1975).

[55] T. J. Liu, X. Ke, B. Qian, J. Hu, D. Fobes, E. K. Vehstedt, H. Pham, J. H. Yang, M. H. Fang, L. Spinu, P. Schiffer, Y. Liu, Z. Q. Mao, Phys. Rev. B **80**, 174509, (2009).

[56] R.C. Dynes, V. Narayanamurti, J.P. Garno, Phys. Rev. Lett. **41**, 1509 (1978).

[57] H. Suhl, B. T. Matthias, and L. R. Walker, Phys. Rev. Lett. **3**, 552 (1959).

[58] W. L. McMillan, Phys. Rev. **175**, 537 (1968).

[59] J.R. Schrieffer, Rev. Mod. Phys. **200**, (1964); J.R.Schrieffer, Theory of Superconductivity, (W.A. Benjamin, New York, 1964).

[60] Y. Noat, T. Cren, F. Debontridder, and D. Roditchev, W. Sacks, P. Toulemonde and A. San Miguel, Phys. Rev. B (2010) (in press).

[61] H. Alloul, J. Bobroff, M. Gabay and P. J. Hirschfeld, Rev. Mod. Phys. **81**, 45-108 (2009).

[62] T. Cren, D. Roditchev, W. Sacks and J. Klein, Europhys. Lett., **54**, 84 (2001); T. Cren, D. Roditchev, W. Sacks, J. Klein, J.-B. Moussy, C. Deville et M. Laguës, Phys. Rev. Lett. **84**, 1 (2000).

[63] A. Maeda, T. Yabe, S. Takebayashi, M. Hase, and K. Uchinokura, Phys. Rev. B **41**, 4112 (1990).

[64] K. Ishida, Y. Kitaoka, N. Ogata, T. Kamino, K. Asayama, J.R. Cooper and N. Athanassopoulou, Physica C **179**, 29 (1991); D. A. Bonn, S. Kamal, Kuan Zhang, Ruixing Liang, D. J. Baar, E. Klein, and W. N. Hardy, Phys Rev. B **50**, 4051 (1994).

[65] Cao Wang, Shuai Jiang, Qian Tao, Zhi Ren, Yuke Li, Linjun Li, Chunmu Feng, Jianhui Dai, Guanghan Cao and Zhu-an Xu, Europhys. Lett. **86** 47002 (2009).

[66] Tristan Cren et al., to be published.

[67] Note that such a low resonance energy of 6 meV would require a very strong electron-magnon coupling if magnon-exchanges where responsible of the pairing mechanism.

[68] J. K. Dong, T. Y. Guan, S. Y. Zhou, X. Qiu, L. Ding, C. Zhang, U. Patel, Z. L. Xiao, and S. Y. Li, Phys. Rev. B **80**, 024518 (2009).

[69] V. G. Tissen, E. G. Ponyatovsky, M. V. Nefedova, A. N. Titov and V. V. Fedorenko, Phys. Rev. B **80**, 092507 (2009).

[70] E. Bellingeri, I. Pallecchi, R. Buzio, A. Gerbi, D. Marrè, M. R. Cimberle, M. Tropeano, M. Putti, A. Palenzona, and C. Ferdeghini, Appl. Phys. Lett. **96**, 102512 (2010).

[71] A. Sow, P. Toulemonde, M. Nùñez-Regueiro, unpublished.

[72] S. C. Lee, E. Satomi, Y. Kobayashi, M. Sato, Phys. Soc. Jpn **79**, 023702 (2010).